Available online at www.sciencedirect.com
SCIENCE DIRECT®

Journal of the European Ceramic Society 23 (2003) 577–584

www.elsevier.com/locate/jeurceramsoc

Kinetic study of the corrosion of silicon nitride materials in acids

J. Schilm, M. Herrmann*, G. Michael

Fraunhofer Institut für keramische Technologien und Sinterwerkstoffe, Winterberg Str. 28, 01277 Dresden, Germany

Received 4 October 2001; received in revised form 6 September 2002; accepted 5 October 2002

Abstract

The leaching behaviour of gas-pressure-sintered silicon nitride materials with different yttria, alumina and silica contents in 1N sulfuric acid at 60–101 °C was studied. The progress of corrosion was investigated in terms of mass loss and thickness of the corroded layer. Dependencies affecting the progression of the corrosive attack, such as the SiO_2 content of the grain boundary phase and the size distribution of the triple junctions, were described. The influence of temperature on the individual stages of the entire process was investigated. First attempts at modelling the complex corrosion behaviour were made. To simplify the mathematical modelling, plates (16 × 16 × 2.5 mm) fulfilling conditions allowing them to be considered as one-dimensional were chosen. Activation energies were calculated for the pure dissolution of the grain boundary phase from mass loss data and from the thickness of the corroded layer. Known solid state reaction models and corrosion models show only a limited ability to describe the investigated system.

Keywords: Acids; Corrosion; Leaching; Si_3N_4

1. Introduction

Silicon nitride, a typical structural ceramic material having superior mechanical properties and chemical stability, has found many applications in severe corrosive environments. It has been successfully applied in the chemical industry in several components, including bearings, ball valves and other armatures. Therefore silicon nitride materials often find application in environments such as acidic or basic solutions at various temperatures. Although ceramics are generally more stable in corrosive environments than are common metallic materials, their chemical resistance under these highly corrosive conditions deserves to be evaluated.

The corrosive behaviour of silicon nitride materials in aqueous media has been the object of extensive study.[1–9,15] However there is still a lack of understanding of the details of the corrosion mechanism in acids. In these investigations it has often been the case that only commercially available materials, with insufficient characterized grain boundary phases, have been used for corrosion experiments. Some papers compared the results obtained for different Si_3N_4 materials or additive systems.[5–7] In only a few papers was the depth of the corrosion layer investigated.[3,7,8] Sometimes the precipitation of reaction products was found to be sensitive to the experimental set-up, due to a high ratio between the surface of the samples and the volume of the solution.[4–6] It has been determined that concentrated acids produce only a small amount of damage in the microstructure of silicon nitride ceramics.[3,6] Some tendencies concerning the relations between corrosion resistance and the microstructure were derived.[10] Despite these facts in all sources remarkable corrosion intensities expressed in different terms have been measured within corrosion periods up to 1000 h. Without a detailed knowledge of the relations between the properties of the material and the medium it is hardly possible to develop corrosion resistant materials.

The corrosion resistance of Si_3N_4 ceramics in acids mainly depends on the amount and composition of the grain boundary phase.[10] The grain size, which is closely related to the size of the triple junctions, is another important factor determining the corrosion resistance of the material. In acidic solutions the grain boundary phase at the triple junctions is mainly attacked and degraded. The network-modifying ions dissolve, while

* Corresponding author.
E-mail address: herrmann@ikts.fhg.de (M. Herrmann).

0955-2219/03/$ - see front matter © 2003 Elsevier Science Ltd. All rights reserved.
PII: S0955-2219(02)00375-8

the network-forming ions remain at least partially in the corroded layer. For this reason it is assumed that a highly hydrated glassy phase remains in the triple junctions. In later stages of the corrosion process, this hydrated glassy network also dissolves in the acid. Fig. 1 shows the corrosive attack schematically. Neither the Si_3N_4 grains nor the intergranular boundary phase (with a thickness of about 1 nm) corrodes significantly.[10] A stable skeleton of silicon nitride grains, exhibiting a residual bending strength of approximately 400–500 MPa, remains.

The corrosion process primarily consists of a dissolution reaction and diffusion-controlled mass transport through the corrosion layer. Under certain conditions a strong decrease in the corrosion rate is observed. These results seem to indicate the presence of additional processes inhibiting degradation. They also suggest that the rate-controlling process changes as corrosion processes.[10,11]

As described above in known literature it has been frequently exposed that acids attack mainly the grain boundary phase, but only less attention has been paid to the influence of the composition of the grain boundary phase on the corrosion behaviour. Thus the aim of this study was to systematically investigate the influence of amount and the composition of the grain boundary phase on the corrosion mechanisms of silicon nitride materials in acids. But it is also focused on problems arising from modelling the complex corrosion process.

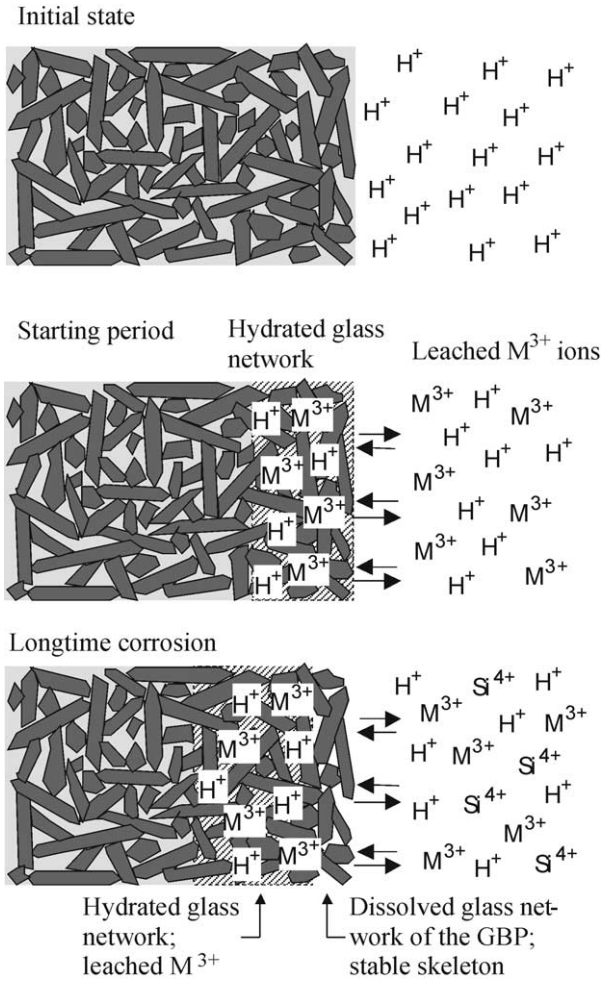

Fig. 1. Schematic view of the corrosive attack on Si_3N_4 containing a glassy grain boundary phase in a diluted acid (except HF).

2. Experimental procedure and materials

Silicon nitride ceramics with different compositions (Table 1) were prepared from Si_3N_4 powder (SNE 10, UBE), Al_2O_3 (AKP50), Y_2O_3 (grade fine, HCST) and SiO_2 (T2 125 Heraeus). The raw powders were suspended in isopropanol and mixed in an attrition mill for 4 h. The powders were dried in a rotavap and granulated using a 400-μm sieve. Bodies of about 100 g (20 × 20 × 70 mm) were formed by cold isostatic pressing (250 MPa). The samples were gas-pressure sintered at 1825 °C to a density of >99.5% of the theoretical density, and after sintering they were cut and ground into slabs having dimensions of 16 × 16 × 2.5 mm. These samples were then used for corrosion testing. The size distribution of the triple junctions was varied by additional heat treatments after the sintering process. The selected temperature was appropriate for obtaining grain coarsening while still maintaining the chemical composition of the grain boundary phase. The amorphous state of the grain boundary phase was verified by XRD.

All corrosion tests were carried out in a 1.5-l PTFE reaction vessel equipped with sample holders made of PP in 1N H_2SO_4. The ratio between the surface of the samples and the volume of the acid was lower than 0.005 m^{-1}. Earlier results and data from the literature [3,5] have shown that diluted acids with a concentration of ca. 1N are highly corrosive for the silicon ceramics of interest. Not more than 20 samples were simultaneously immersed in the acid. The solutions were continuously stirred and completely changed after certain times to avoid precipitation of reaction products. This setup and the procedure of conducting the corrosion tests was chosen to avoid experimental disadvantages, which have

Table 1
Compositions of the grain boundary phases of the investigated materials

Sample	Y_2O_3 (wt.%)	Al_2O_3 (wt.%)	SiO_2 (wt.%)	SiO_2 (grain boundary) (wt.%)	Overall amount of additives (wt. %)
SiN 1	6	4.0	2.7	22	12.7
SiN 2	6	4.0	4.1	29	14.1
SiN 3	6	4.0	5.6	36	15.6
SiN 4	4	2.7	4.7	42	11.4
SiN 5	4	2.7	2.6	28	9.3
SiN 6	8	5.3	5.5	29	18.8

been found in the reviewed literature. A Lauda thermostat filled with silicone oil was used to heat the vessel. The desired temperature was maintained within a range of ±0.5 K. A balance with an accuracy of ±10 μg was used to measure the mass loss. The thickness and morphology of the corroded layer were investigated microscopically and determined by quantitative image analysis (Image Tool v2). The size distributions of the triple junctions were measured by quantitative image analysis of SEM images (Quantimed 5000).

3. Results

3.1. Temperature dependence

The specific mass loss on the surface and the corrosion layer thickness for material SiN2 at various temperatures are shown in Fig. 2a and b. At low temperatures (60 °C) the results show a linear behaviour, indicating that the progress of acidic attack is completely interfacial- or reaction-controlled. With increasing temperature of the solution, linear behaviour is exhibited only in the initial stage of corrosive attack. The rate of corrosion decreases in the subsequent stage, indicating that the corrosion process becomes diffusion-controlled. Application of temperatures of 90 °C and higher causes the corrosive attack to cease almost completely after about 120 h. It is assumed that this occurs due to an "in situ" passivation reaction occurring inside the corroded layer. Due to the planar character of the samples (16 × 16 × 2.5 mm) this extreme behaviour cannot be explained by a shrinking core effect. Optical micrographs show (Fig. 3a–c) the development of the corrosion layer at 90 °C. The appearance of two different corrosion layers in Fig. 3c can be seen clearly. It is assumed that the outer corrosion layer results from the dissolution of the hydrated SiO_2 phase. Attention must be paid to the results measured at 101 °C: These data show that passivation starts earlier at a lower mass loss than it does at 90 °C. Because the passivation reaction does not occur at lower temperatures, the overall destruction intensity at those lower temperatures is greater than at higher temperatures. Temperature dependencies as described have been found for all investigated materials with a SiO_2 content of less than 29% by weight in the grain boundary phase.

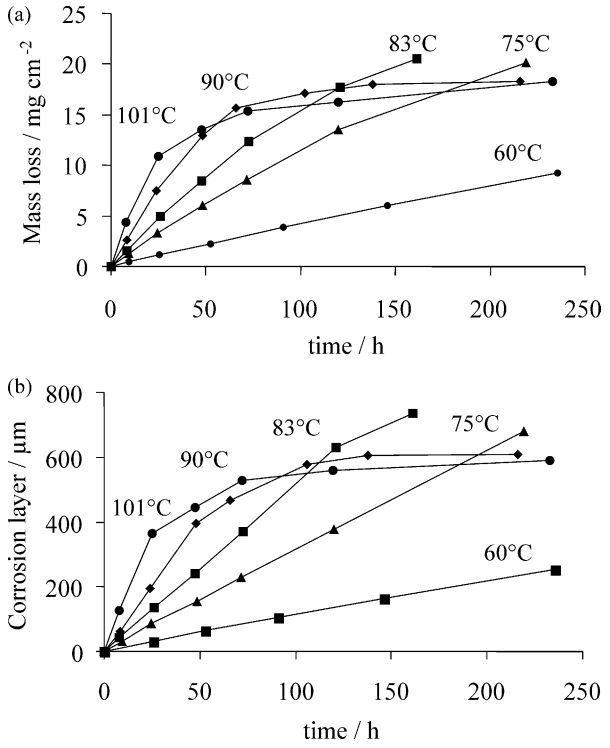

Fig. 2. Time-dependent mass loss (a) and thicknesses of corrosion layer (b) of SiN 2 in 1N sulfuric acid at various temperatures.

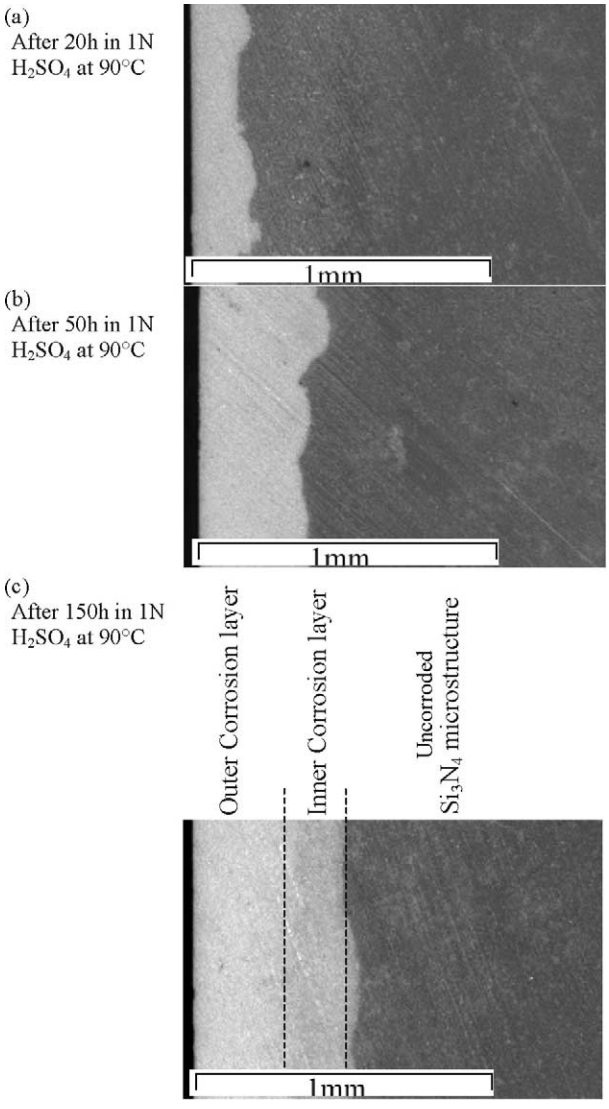

Fig. 3. (a–c) Optical micrographs of cross-sections of Si_3N_4 samples after different corrosion times.

3.2. Activation energies

For three out of five ceramics investigated, the activation energies for the initial dissolution of the grain boundary phase were determined from mass loss data and corrosion layer thickness. The activation energies were calculated from the slopes of Arrhenius plots and are presented in Fig. 4a. The data were taken from the initial linear parts of plots as shown for example for SiN2 in Fig. 2a and b. To calculate the kinetic constant (k_R) at each temperature the equation $\alpha(t) = k_R \cdot t$ was used. The activation energies were determined by least squares fits (Fig. 4b).

R^2 values obtained for linear regression analysis are usually greater than 0.99. This is a strong indication that the initial corrosion stage is reaction-controlled. The values of the activation energies range from 50 to 65 kJ mol^{-1}.

3.3. SiO_2 content of grain boundary phase

In the field of glass corrosion, it is known that the SiO_2 content is mainly responsible for corrosion resistance in acidic environments. As can be seen in Table 1, silicon nitride ceramics SiN1–4 were prepared with different the SiO_2 concentrations in the grain boundary phase. The maximum SiO_2 content of the grain boundary phase is limited by the crystallization of oxynitrides, which results in grain boundary phase with low SiO_2 contents[18].

The results obtained from corrosion experiments at 90 °C are presented in Fig. 5a and b. Comparison of the two figures shows that mass losses and corrosion layer thickness are interrelated. Several remarkable facts can be elucidated from these figures. For the initial stage of the corrosion process, the known facts from glass science can be confirmed. With an increasing SiO_2 content of the grain boundary phase, the numerical value of the reaction rate constant k_R decreases. Additionally only ceramic materials having comparably low SiO_2 contents (SiN1 and SiN2) in the grain boundary phase show passivation behaviour. SiN3 and SiN4 exhibit only reaction- or interfacial-controlled corrosion behaviour, with lower reaction rates in the investigated period of time.

3.4. Size distribution of the triple junctions

Due to the fact that for prolonged corrosion experiments the corrosion rate can be rate-controlled by diffusion of the leached ions and the formation of a passivation layer, influencing the mass transport inside the corrosion layer, the overall corrosion rate could be also influenced by the size and distribution of the triple junctions. The size of the triple junctions, which is closely connected to the grain size, was varied by additional heat treatments of the ceramics. The measured size distributions of the investigated materials are shown in Fig. 6.

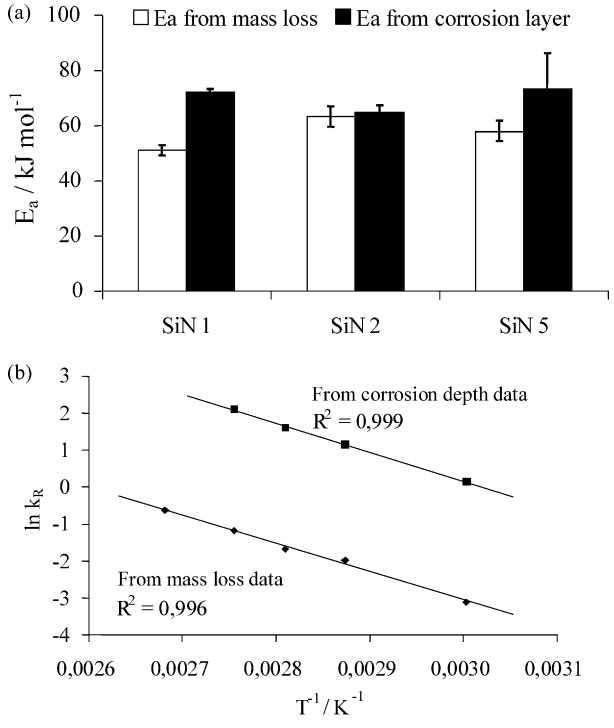

Fig. 4. (a) Activation energies for the dissolution process of the grain boundary phase in several ceramics calculated from mass loss data and corrosion layer thickness. (b) Example illustrating the temperature dependence of rate constants on the dissolution of the grain boundary phase; values are obtained from the linear section of the time-dependent mass loss data and the corrosion layer thickness (material SN).

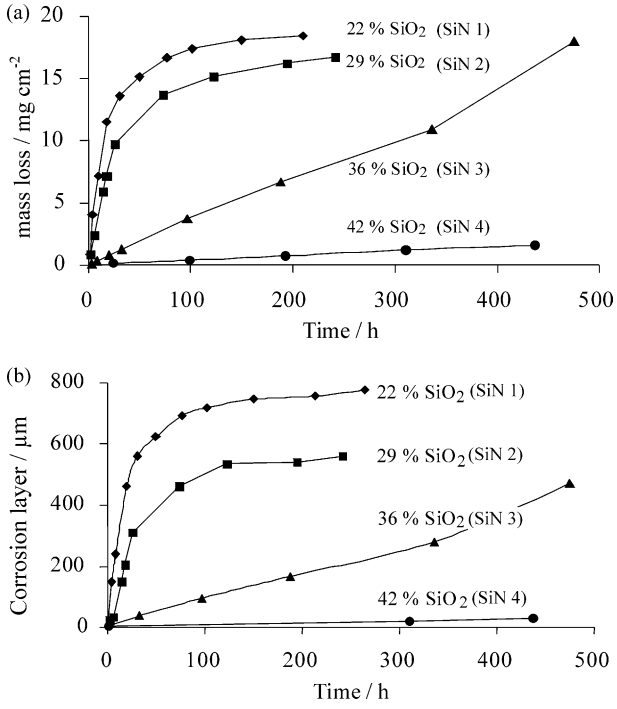

Fig. 5. Time-dependent mass loss data (a) and thicknesses of corrosion layer (b) for various ceramics containing different amounts of SiO_2 in the grain boundary phase at 90 °C in 1N sulfuric acid.

Samples were corroded at temperatures of 60 and 90 °C; the results are presented in Fig. 7. It can be clearly seen that for both temperatures, the data in the linear ranges, rate-controlled by a chemical reaction, coincide well. This indicates that the chemical composition of the grain boundary phase was not changed by the heat treatment. A discrepancy appears in the subsequent stages at 90 °C, where the corrosion process is rate-controlled by mass transport and passivation. Compared with SiN 2, the material SiN 2a, having a larger triple junction size, exhibits a higher overall mass loss and a passivation reaction that occurs later.

3.5. Amount of grain boundary phase

The corrosion behaviour of three materials with similar SiO_2 contents but different amounts of grain boundary phase was investigated. The measured mass loss data and thickness of the corroded layers are presented in Fig. 8. It must be noticed that the mass loss data are standardized by the fractions of grain boundary phase in the materials, which are listed in Table 1. The initial linear corrosion rates of the three materials coincide well, even when it is regarded that SiN5 has a slightly lower SiO_2 content. With increased corrosion attack the corrosion rates start to diverge indicating that the passivation process occurs at later stages when the amount of grain boundary phase rises. High amounts of grain boundary phase lead to deeper corrosion layers (Fig. 8b).

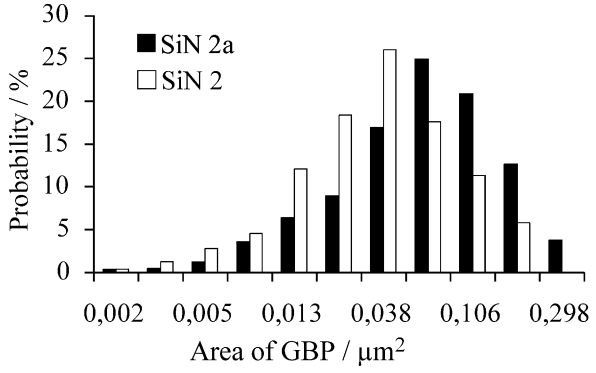

Fig. 6. Comparison of the size distributions of the triple junctions of SiN 2 and SiN 2a (produced by heat treatment of SiN2); the grain boundary phase of the heat-treated material SiN 2a shows a coarsened structure.

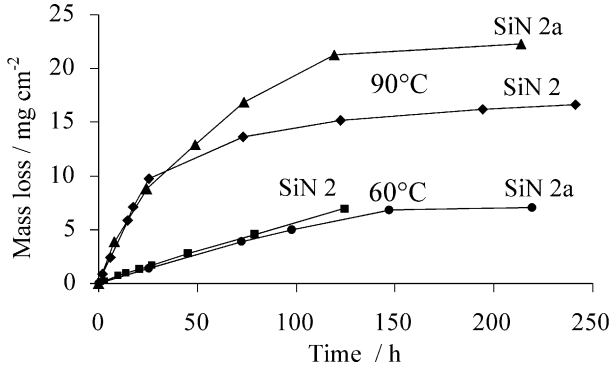

Fig. 7. Mass loss data for the ceramics SiN 2 and SiN 2a at 60 and 90 °C in 1N sulfuric acid; SiN 2a differs from SiN 2 in that it underwent an additional heat treatment in order to force grain coarsening to occur.

4. Discussion

The results described here suggest a division of the entire corrosion process into three stages, shown schematically in Fig. 9. Simple laws can characterize each of these stages individually:

I. Reaction-controlled dissolution of the grain boundary phase

$$\alpha(t) = k_R \cdot t \quad \text{for a low corrosion layer thickness} \tag{1}$$

II. Diffusion-controlled mass transport through the corrosion layer

$$\alpha(t) = k_D \cdot \sqrt{t} \quad \text{for medium corrosion layer thickness} \tag{2}$$

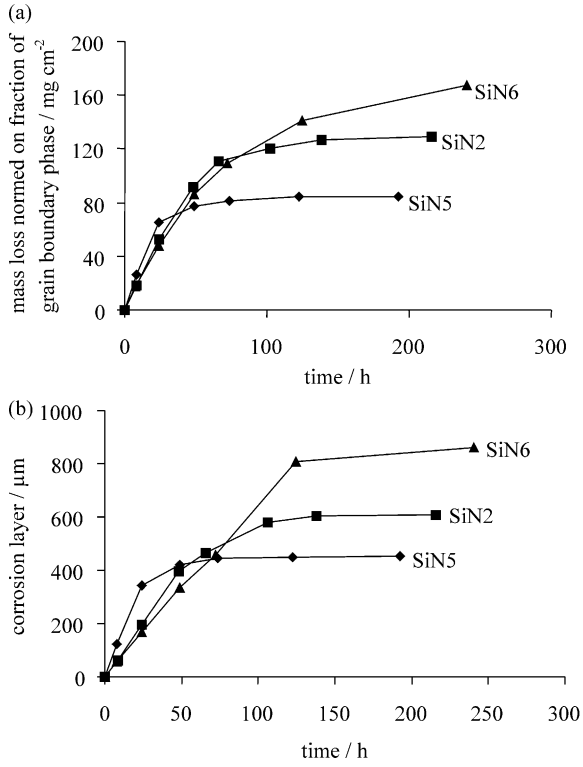

Fig. 8. Time-dependent mass loss data (a) and corrosion layer thicknesses (b) for various ceramics containing different amounts of grain boundary phases with similar SiO_2 contents at 90 °C in 1N sulfuric acid (amount of grain boundary phase: SiN6: 18.8; SiN2: 14.1; SiN5: 9.3 wt.–%).

III. "In situ" passivation inside the corrosion layer, implying a very strong decrease of the corrosion rate up to 0

$$a(t) \rightarrow \alpha_P \approx \text{const for } t >> 0 \quad (3)$$

In these equations, k_R and k_D represent rate constants and $\alpha(t)$ describes the time-dependent conversion of the sample. Normally the value of α ranges from 0 to 1 and is defined by the expressions.

$$\alpha = \frac{\Delta m}{\Delta m_{max}} \text{ or } \alpha = d_{corr}/d_{corr.max} \quad (4)$$

Because Δm_{max} is difficult to determine, in this study α is given in units of mg/cm^2 and μm. The constants depend not only on temperature but also on the amount and composition of the grain boundary phase. Additionally the type and concentration of the acid used have a significant influence on the value of the constants. Each of these rate equations is valid for samples with a one-dimensional geometry and can be applied only in the range of an individual stage of the whole process. These boundary conditions can be applied to the samples used in this study. The geometry of the bending bar used in most of the experiments results in a reduction of the reaction rate without a change of the mechanism (shrinking core models). This makes the distinction between the different mechanisms and the observation of passivation much more complicated as in the case of planar samples chosen in our experiments. Taking the principles of the corrosive attack of Si_3N_4 ceramics into consideration, it would appear reasonable to adopt models from glass corrosion, describing the leaching behaviour in acids, for the investigated materials. The literature on glass corrosion shows that a combination of the first two equations is used to describe similar corrosion processes [Eq. (5)].

$$\alpha(t) = k_R \cdot t + k_D \cdot \sqrt{t} \quad (5)$$

This model can be deduced from the general diffusion equation and is of use in characterizing the corrosion behaviour of glasses.[11] The two terms describe the interfacial-controlled dissolution of glass, i.e., the grain boundary phase and the diffusion-controlled mass transport of the leached components. Another model [Eq. (6)], was derived from the universal mass balance for "mixed reaction control".[12,16] The model was applied, for example, by Conradt [13] and Kuhn [14] to characterize the leaching behaviour of nuclear waste glasses. In Eq. (6), "a" and "b" are simplified constants that represent the properties of the modelled system.

$$\alpha(t) = \sqrt{a \cdot t + b^2} - b \quad (6)$$

This equation is only valid for the first two stages of the observed corrosion process (Fig. 9). In Fig. 10a the presented models were applied to fit the entire corrosion process. The numerical results for the constants of each equation are listed in Table 2. While Eq. (6) is obviously unsuitable, Eq. (5) fits the experimental data well, at least from a mathematical point of view. Upon closer examination of the numerical results for the rate constants, however, the physical senselessness of the model is proven: The regression analysis yields a negative value for k_R.

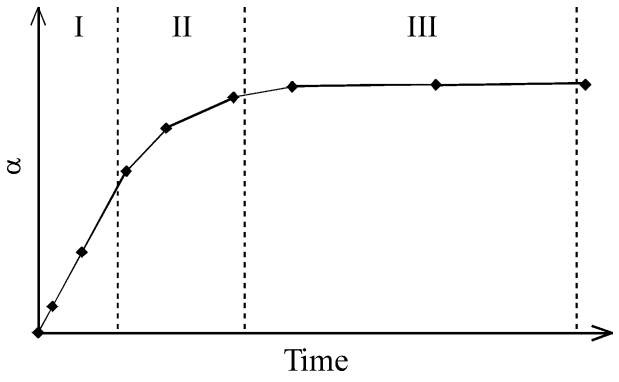

Fig. 9. Schematic showing separation of the entire corrosion process into stages (I) dissolution of the grain boundary phase; (II) diffusion-controlled section; and (III) "in situ" passivation.

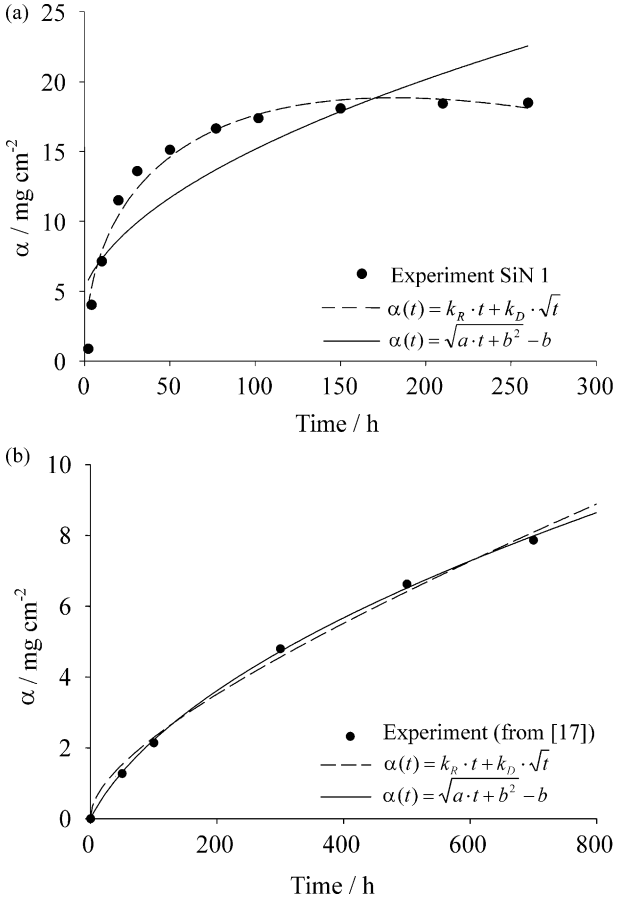

Fig. 10. Regression analysis with different models of corrosive attack for a silicon nitride ceramic containing a glassy Y_2O_3–Al_2O_3–SiO_2 grain boundary phase (a) and a material containing MgO–Al_2O_3–SiO_2 grain boundary phase (b); for details of this material, see Ref. [17].

Table 2
Numerical results for regression analysis of the corrosion behaviour of a Si_3N_4 ceramic with an Y_2O_3–Al_2O_3–SiO_2 glass as the grain boundary phase, material SN (α in mg/cm^2, time in h)

Equation	R^2	k_R;a	k_D;b
$\alpha(t) = k_R \cdot t + k_D \cdot \sqrt{t}$	0.96	-0.1 ± 0.01	2.8 ± 0.2
$\alpha(t) = \sqrt{a \cdot t + b^2} - b$	0.75	1.5 ± 0.4	-2.6 ± 1.0

Table 3
Results for numerical regression analysis of the corrosion behaviour of a Si_3N_4 ceramic with an MgO–Al_2O_3–SiO_2 glass as the grain boundary phase, described in Ref. [10] (α in mg/cm^2, time in h)

Equation	R^2	k_R;a	k_D;b
$\alpha(t) = k_R \cdot t + k_D \cdot \sqrt{t}$	0.995	0.005 ± 0.001	0.2 ± 0.03
$\alpha(t) = \sqrt{a \cdot t + b^2} - b$	0.999	0.013 ± 0.008	1.9 ± 0.3

Nevertheless to prove that these models are not generally unsuitable for describing the corrosion behaviour of silicon nitride materials, they were applied to the corrosion data of materials prepared with a Mg–Al–Si glass as the grain boundary phase.[10] The graphical results are provided in Fig. 10b; the numerical results for the constants, in Table 3. It can clearly be seen that the results fit the experimental data well and that the positive values of the constants also make sense from a physical point of view.

These data illustrate the need for an appropriate kinetic model for lifetime prediction. A model that is able to describe the whole corrosion process, including the passivation reaction, is missing. The complexity of the problem suggests numerical solution of the differential equations with appropriate boundary conditions and a minimum of adjustable parameters.

The measured activation energies are comparable with the results obtained by Ref. 1 from corrosion experiments 1M HCl. Slightly lower activation energies were calculated by Ref. 5 using 8.5M HCl for corrosion tests. The discrepancies between the values obtained from mass loss data and depth of the corroded layer can be connected with the onset of formation of the SiO_2 protective layer or even with a decelerated leaching rate of at least one component of the grain boundary phase. The calculated activation energies and the determined reaction constants for the initial reaction period allow predicting the corrosion rate at lower temperatures. The corrosion rates at room temperature are 12–40 times lower than at 60 °C (Table 4).

At temperatures of 90 °C and higher, a strong decrease in the corrosion rate due to structural changes inside the corrosion layer results. Whether or not this behaviour can be used to attain permanent protection against corrosive attack without a significant reduction in the mechanical properties must be clarified further.

Table 4
Predicted corrosion rates at low temperatures, assuming completely reaction-controlled behaviour

Material	k (mg cm^{-2} h^{-1}) at 60 °C	k (mg cm^{-2} h^{-1}) at 20 °C	k (μm h^{-1}) at 60 °C	k (μm h^{-1}) at 20 °C
SiN 1	0.16	0.013	4.3	0.12
SiN 2	0.05	0.002	1.2	0.05
SiN 5	0.06	0.003	0.9	0.02

This could possibly be achieved through formation of the protective layer in an early stage of the corrosion process. It is important to note that the temperature range between 60 and 90 °C seems to be critical due to the remarkably high corrosion rates and a missing passivation reaction in this range. This fact necessitates testing of the durability of the protective layers in this temperature range.

The results clearly show that higher SiO_2 concentrations in the grain boundary phase lead to a decrease of nearly two orders of magnitude in the dissolution rate of the grain boundary phase. Because the corrosion rate of SiN3 (Fig. 5) does not cease, it can be assumed that in an early stage of the entire process, a corrosion layer with a finite thickness must exist before a passivation reaction occurs. The relation of this behaviour with the composition of the grain boundary phase, especially the SiO_2 content, has to be explored in further studies.

On the bases of the experimental results (Figs. 7 and 8) some conclusions about the influence of the size of the triple junctions on the corrosion can be drawn. The results show, that in the initial reaction period (interface control) no influence could be observed but the passivation reaction occurs later and at a significantly higher mass loss in materials with a coarser triple junctions phase (SiN 2a) than in materials with the finer triple junctions (SiN2). Such behaviour is in agreement with the proposed model for the formation of passivation layers. Through tailoring of the microstructure to produce finer triple junctions, i.e., through the use of smaller Si_3N_4 grains or lower additive contents, the corrosion behaviour can be improved significantly.

Additionally the effect of the amount of the grain boundary phase on the corrosion process can be monitored. The reduction of the amount of additives has the same effect as the reduction of the size of the triple junctions. When the SiO_2 content is not controlled than the reduction of additives normally result in an increase of the SiO_2 content causing also an increase in the corrosion resistance.

5. Conclusions

The results show clearly that the overall corrosion process of silicon nitride ceramics consists of at least three different processes superimposing on each other.

Each of these processes can be rate controlling, but every single corrosive attack starts with an interfacial-controlled dissolution reaction, evidenced by the accuracy of the calculated activation energies. The corrosion rates at temperatures lower than 60 °C can be predicted from Arrhenius plots. The extent to which each individual process is rate controlling depends on several parameters:

1. Temperature and concentration of the acids;
2. Depth of the corrosion layer;
3. SiO_2 content of the Grain boundary phase; and
4. Size distribution of the triple junctions.

The temperature dependence shows how enormously the corrosion behaviour changes over a temperature range spanning 40 K. Based on known results, a certain thickness of the corroded layer seems to be necessary for the formation of a protective layer. The SiO_2 content of the grain boundary phase is one of the most important parameters influencing corrosion resistance in acids. Through an increase in the SiO_2 content from 22 to 42%, the initial corrosion rate can be reduced by more than two orders of magnitude. Models that consider only reaction control or mass transport are unsuitable for describing the entire corrosion process. Even more complex models that consider a mixed reaction control are not appropriate.

Acknowledgements

This work was supported by the DFG under contract number HE2471/1.

References

1. Sato, T., Tokunaga, Y., Endo, T., Shimada, M., Komeya, K., Komatsu, M. and Kameda, T., Corrosion of silicon nitride ceramics in aqueous hydrogen chloride solutions. *J. Am. Cer. Soc.*, 1988, **71**(12), 1074–1079.
2. Sato, T., Tokunaga, Y., Endo, T., Shimada, M., Komeya, K., Komatsu, M. and Kameda, T., Corrosion of silicon nitride ceramics in aqueous HF solutions. *J. Mat. Sci.*, 1988, **23**, 3440–3446.
3. Iio, S., Okada, A., Asano, T. and Yoshimura, M., Corrosion behaviour of silicon nitride ceramics in aqueous solutions (Part 3). *J. Cer. Soc. Japan, Int. Edition*, 1992, **100**, 954–957.
4. Shimada, M. and Sato, T., Corrosion of silicon nitride ceramics in HF and HCl solutions. *Ceram. Trans. Symp.*, 1990, **10**, 355–365.
5. Sharkawy, S. W. and El-Aslabi, A. M., Corrosion of silicon nitride ceramics in aqueous HCl and HF solutions at 27 °C–80 °C. *Corrosion Science*, 1998, **40**(7), 1119–1129.
6. Bellosi, A., Graziani, T. and Monteverde, F., Degradation behaviour of silicon nitride in aqueous acid solutions. *Key Engin. Mat.*, 1996, **113**, 215–226.
7. Kanbara, K., Uchida, N., Uematsu, K., Kurita, T., Yoshimoto, K. and Suzuki, Y., Corrosion of silicon nitride ceramics by nitric acid. *Mat. Res. Soc. Symp. Proc.*, 1993, **287**, 533–538.
8. Okada, A. and Yoshimura, M., Mechanical degradation of Silicon nitride ceramics in corrosive solutions of boiling sulphuric acid. *Key Engin. Mat.*, 1996, **113**, 227–236.
9. Monteferde, F., Mingazzini, C., Giorgi, M. and Bellosi, A., Corrosion of silicon nitride in sulphuric acid aqueous solution. *Corrosion Science*, 2001, **43**, 1851–1863.
10. Herrmann, M., Schilm, J., Michael, G., Meinhardt, J. and Flegler, R., Corrosion of Silicon Nitride materials in acidic and basic solutions and under hydrothermal conditions; *J. Eur. Ceram. Soc.*, 2003, **23**, 585–594.
11. Seipel, B. and Nickel, K., G., Corrosion of silicon nitride in acidic solutions: Penetration monitoring. *J. Eur. Ceram. Soc.*, 2003, **23**, 595–602.
12. Frade, J. R. and Cable, M., Theoretical solutions for mixed control of solid state reactions. *J. Mat. Sci.*, 1997, **32**, 2727–2733.
13. Conradt, R., Roggendorf, H. and Scholze, H., A contribution to the modelling of the corrosion process for HLW glasses. *Mat. Res. Soc. Symp. Proc.*, 1985, **44**, 155–162.
14. Kuhn, W. L., Peters, R. D. and Simonson, S. A., Development of a leach model for nuclear wastes glass. *Nuclear Technology*, 1983, **63**, 82–89.
15. McCauley, R., A., *Corrosion of Ceramics*, Vol. 1. Marcel Dekker, 1995.
16. Frade, J. R. and Cable, M., Reexamination of the basic theoretical model for the kinetics of solid-state reactions. *J. Am. Ceram. Soc.*, 1992, **75**, 1949–1957.
17. Herrmann, M., Schilm, J., Michael, G. and Meinhardt, J., DFG Report HE2457/2-4, 2000.
18. Wötting, G., Herrmann, M., Michael, G., Siegel, S. and Frassek, L., WO99/20579, 1999.